Journal of Applied Physics

RESEARCH ARTICLE | OCTOBER 18 2007

Beryllium deposition on International Thermonuclear Experimental Reactor first mirrors: Layer morphology and influence on mirror reflectivity

G. De Temmerman; M. J. Baldwin; R. P. Doerner; D. Nishijima; R. Seraydarian; K. Schmid; F. Kost; Ch. Linsmeier; L. Marot

Journal of Applied Physics 102, 083302 (2007)
https://doi.org/10.1063/1.2798389

Beryllium deposition on International Thermonuclear Experimental Reactor first mirrors: Layer morphology and influence on mirror reflectivity

G. De Temmerman,[a] M. J. Baldwin, R. P. Doerner, D. Nishijima, and R. Seraydarian
Center for Energy Research, University of California at San Diego, La Jolla, California 92093, USA

K. Schmid, F. Kost, and Ch. Linsmeier
EURATOM Association, Max-Planck Institut für Plasmaphysik, D-85748, Garching b. München, Germany

L. Marot
Institute of Physics, University of Basel, CH-4056 Basel, Switzerland

(Received 27 July 2007; accepted 30 August 2007; published online 18 October 2007)

Metallic mirrors will be essential components of the optical diagnostic systems in the International Thermonuclear Experimental Reactor (ITER). Reliability of these systems may be affected by mirror reflectivity changes induced by erosion and/or deposition of impurities (carbon, beryllium). The present study aims to assess the effect of beryllium (Be) deposition on the reflectivity of metallic mirrors and to collect data on the optical quality of these layers in terms of morphology, roughness, etc. Mirrors from molybdenum and copper were exposed in the PISCES-B linear plasma device to collect eroded material from graphite and beryllium targets exposed to beryllium-seeded deuterium plasma. After exposure, relative reflectivity of the mirrors was measured and different surface analysis techniques were used to investigate the properties of the deposited layers. Be layers formed in PISCES-B exhibit high levels of porosity which makes the reflectivity of the Be layers much lower than the reflectivity of pure Be. It is found that if Be deposition occurs on ITER first mirrors, the reflectivity of the coated mirrors will strongly depend on the layer morphology, which in turn depends on the deposition conditions.
[DOI: 10.1063/1.2798389]

I. INTRODUCTION

Plasma diagnostic systems will be necessary tools for the future success of the International Thermonuclear Experimental Reactor (ITER) both to better understand the physics involved in magnetically confined burning plasmas[1] and for the protection of the device in case of disruptions or any other unforeseen adverse operating scenarios. Contrary to today's tokamaks, the high radiation levels and neutron fluxes expected in ITER prevent the direct observation of the plasma through optical windows or fibers, which are subject to radiation-enhanced effects such as luminescence and absorbance. Therefore, it has been proposed that the plasma light/radiation will be transmitted by metallic mirrors (called first mirrors) to diagnostics via a labyrinth embedded in the shielding material.[2]

Due to its proximity to the hot confined plasma, the first mirror surface is expected to suffer from erosion by charge-exchange neutrals and/or redeposition of impurities that are eroded from the plasma-facing components.[3,4] Experiments aimed at studying the deterioration of the mirror reflectivity induced by these damaging effects have been initiated both in the laboratory[5–7] and in tokamaks.[8–10] In these experiments, only the effect of carbon deposition on the mirror surface was considered and was found to lead to a significant decrease of the mirror reflectivity even for very thin deposited layers (around 10 nm).[3] However, not only carbon, but also beryllium deposition, may be expected on ITER first mirrors.

Because of the combination of materials to be used in ITER and the choice of beryllium as a first wall material in the main chamber, the scrape-off layer plasma flow in the divertor may contain a significant fraction of beryllium.[11] Experiments in the PISCES-B divertor-plasma simulator have shown that even with a very low fraction of beryllium ions in the plasma ($\approx 0.1\%$), at plasma parameters relevant to ITER, a graphite target becomes coated with a beryllium layer that reduces its erosion by the plasma.[12,13] In turn, Be re-erodes and leads to the formation of Be-rich layers in line-of-sight locations from the target. Unlike carbon which can migrate and be deposited in plasma-shaded areas, long-range migration is not expected for beryllium. Thus, the study of the impact of beryllium deposition on first mirror reflectivity is of considerable interest and is especially vital to supplement the lack of such data. With the exception of the first mirror test initiated at JET,[14] where the carbon first wall is regularly coated with beryllium, no experimental data are currently available on this topic. The present study aims at assessing the effect of Be layers formed in PISCES-B on the reflectivity of metallic mirrors and collecting data on the optical quality of these layers in terms of their resultant morphology, roughness, etc.

II. EXPERIMENTAL

PISCES-B is a linear plasma device. The plasma can be operated continuously in steady-state conditions and is gen-

[a]Electronic mail: gdetemmerman@ucsd.edu

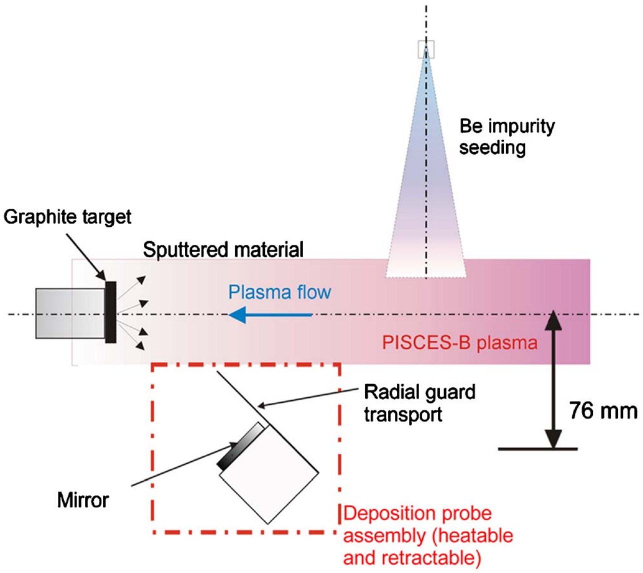

FIG. 1. (Color online) Arrangement used to collect deposited/codeposited material during exposure of metallic mirrors in PISCES-B.

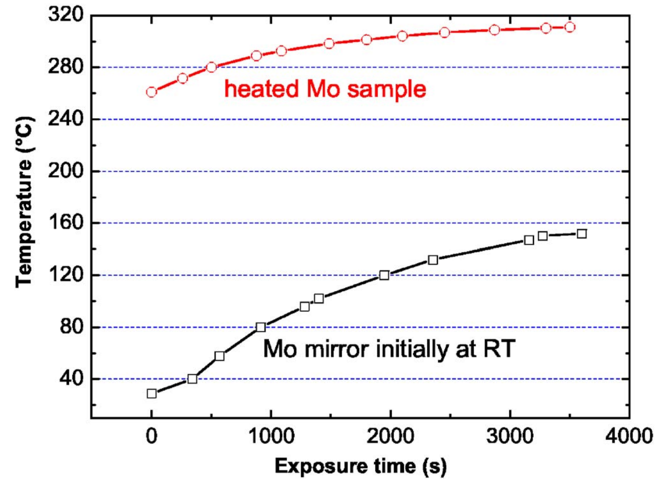

FIG. 2. (Color online) Evolution of the mirror temperature during plasma exposure, for heated and nonheated mirrors. The increase in the mirror temperature with time is due to the surface heating by the plasma.

erated by an arc discharge initiated with a heated LaB_6 cathode. The anode and axial magnetic field define cylindrical plasma with a diameter of about 50 mm and axial length greater than 1 m. The machine is installed in an airtight enclosure to allow safe operations with beryllium.[15]

Figure 1 schematically shows the experimental arrangement used, which is described in more details elsewhere.[13] Graphite, or beryllium, targets are exposed to a high-flux deuterium plasma ($\sim 3\times 10^{22}$ ions $m^{-2}\ s^{-1}$). A Be impurity flux in the plasma is generated through the use of an evaporative atomic beam source (Veeco/Applied EPI molecular beam source). The emerging atom beam is oriented in such a way[16] that the beam travels perpendicular to the magnetic axis of the machine. The plasma parameters used here ($n_e \sim 2-3\times 10^{18}\ m^{-3}$ and $T_e=6-10$ eV) are sufficient to ionize the injected Be atoms once they enter the plasma. The beryllium ions thus created are entrained by the plasma flow toward the target. The concentration of beryllium ions in the plasma is controlled by varying the temperature of the evaporator oven and is measured spectroscopically using the method described in Ref. 17.

A negative bias of −50 V is applied to the target to control the impinging ion energy. In the case of graphite targets, the target temperature was about 700 °C to simulate the working temperature of ITER strike points. When a beryllium target was used, its temperature was maintained at about 30 °C by water cooling.

Mirrors made of either molybdenum or copper were used for the experiments. The initial roughness of the samples was in the range 15–20 nm for Mo and 10–15 nm for Cu. The mirrors were installed on a movable witness plate manipulator (Fig. 1) to collect eroded material during the targets exposure to the plasma. The mirrors were shielded from cross-field plasma transport so that only particle fluxes from sputter-erosion and reflection from the target contribute to deposition. The witness plate can be independently heated and is fully retractable into a vacuum interlock chamber to allow sample replacement. During exposure to the plasma, the witness plate temperature increases by about 100 °C h^{-1}, for a sample initially at room temperature, due to heating by the plasma radiation. Experiments were made with two different initial temperatures: 20 and 240 °C. Evolution of the temperature is followed by a thermocouple installed at the backside of the mirror. Figure 2 shows the evolution of a Mo mirror temperature during a typical exposure. For a nonheated mirror the temperature varies between 25 and 150 °C, while it varies between 260 and 310 °C for a heated mirror.

An important issue with mirrors is the evaluation of their optical reflectivity. In the present case, the presence of beryllium on mirrors necessitated a simple reflectance measurement compatible with beryllium handling. A schematic drawing of this setup is shown in Fig. 3. After exposure, each mirror is removed from the machine and installed on a sample holder located inside the PISCES-B beryllium enclosure, the mirror surface is parallel to the enclosure window. Outside the enclosure, a calibrated white light source (Optronics spectral radiance lamp) illuminates the sample with an incidence angle of about 10°. The reflected light is collected by a lens, and guided by an optical fiber to a spectrometer equipped with a linear charge coupled device array (Ocean Optics USB4000). Measurements are done in the wavelength range 400–1000 nm. To avoid the necessity of

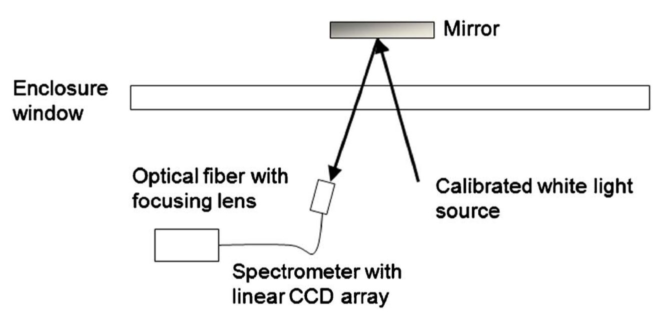

FIG. 3. (Color online) Schematic drawing of the setup used for reflectivity measurements on mirrors exposed in PISCES-B.

TABLE I. Experimental conditions for the mirror exposures made in PISCES-B. The indicated film thicknesses were determined by NRA measurements. c_{Be} is the beryllium ion fraction in the plasma and R_a is the arithmetic surface roughness measured with a profilometer.

Mirror	Temperature (°C)	c_{Be} (%)	Film thickness (nm)	Deposition rate (nm s^{-1})	R_a (nm)
W	250–300	0.15	90	0.025	40.6
Cu	250–310	0.05	75	0.02	16
Cu	250–310	0.1	55	0.015	14.3
Cu	250–310	0.03	15	0.004	19.6
Cu	RT-150	0.09	41	0.011	21.9
Cu	RT-150	0.05	41	0.011	11.3
Mo	250–310	0.05	3.5	8.3×10^{-4}	11.3
Mo	250–310	0.05	5	0.001	17.9
Mo	250–310	0.05	55	0.015	7.6

using a calibrated sample for the determination of the absolute reflectance, the relative reflectivity of the exposed mirrors was measured. This is defined by

$$R_{rel} = \frac{I_{exposed}}{I_{reference}}, \tag{1}$$

where $I_{exposed}$ is the intensity measured at a given wavelength, when an exposed mirror is placed on the sample holder, and $I_{reference}$ is the same measurement done with a nonexposed mirror made from the same material. To complement these data, surface analysis on the exposed mirrors were made in IPP Garching by sputter-depth profiling x-ray photoelectron spectroscopy (XPS) to determine the deposited film composition, and nuclear reaction analysis (NRA) to determine the layer thickness. Surface morphology of the samples was studied by means of a JEOL-JSM 6830 scanning electron microscope (SEM), while arithmetic surface roughness (R_a) was measured with a Dektak IIA stylus profilometer. The scan length was 200 μm and five scans were made at different locations on the sample surface. The arithmetic roughness is defined as the arithmetic average of the absolute values of the measure profile height deviations taken within the sampling length and measured from the graphical center line.

III. RESULTS

A. Layer thickness and composition

The typical plasma exposure time used in this study was 1 h. Table I summarizes the experimental conditions used for the mirror exposures, as well as the film thickness and roughness measured on the mirrors after exposure. After exposure, all samples were found to be coated with a dark Be film of thickness ranging from 15–90 nm, depending on the exposure conditions. According to XPS sputter-depth profiles, the deposited layers consist mainly of beryllium with some amount of oxygen (about 10%) and carbon concentrations of less than 3%. This is consistent with the results described in Ref. 13, where a small Be fraction in the plasma (between 0.03% and 0.15% in the present case) leads to the formation of Be-rich codeposited films in line-of-sight locations from the graphite target. The deposited layers exhibit a low roughness and the formation of the beryllium layer does not lead to a significant change of the mirror roughness as expected given the relatively small film thicknesses studied here. Moreover, the substrate temperature during the exposure does not seem to influence the roughness of the deposited film. For the experimental conditions described in this paper, the deposition rate of beryllium on the mirrors was found to be in the range 0.001–0.025 nm s^{-1}. It should be noted that the deposition rate was found to be independent of the mirror temperature as expected given that the melting temperature of beryllium is 1270 °C. Contrary to what is observed for carbon, for which an increase of the surface temperature decreases the deposition rate on the mirror by enhancing the chemical erosion of carbon by deuterium[18] from the coated mirror surface, no such effect should be expected in the case of Be deposition.

B. Influence of beryllium deposition on mirror reflectivity

For all the experimental conditions investigated here, the mirrors did not exhibit the shiny gray appearance that is typical for a bulk beryllium polished sample. Instead, the Be films appear dark but at the same time rather reflective (an image is still reflected by the surface). The aspect of the layer changes when the sample is rotated from normal incidence, which is usually an indication for a highly oriented surface morphology.

Figure 4 shows relative reflectivities measured on both the molybdenum and copper mirrors after exposure. In both cases, the mirrors were heated during the exposure. For the molybdenum mirrors [Fig. 4(a)], the thicker the Be layer, the lower the reflectivity. A 3.5 nm thick film does not significantly affect the reflectivity (Be and Mo have close reflectivity values in the wavelength range of interest[19]), a reflectivity drop of about 30% at $\lambda=400$ nm is measured for a 5 nm Be film, while the relative reflectivity falls to 30% at $\lambda=400$ nm for a 60 nm film.

For the case of the copper mirrors [Fig. 4(b)], a different behavior is observed. Contrary to what is observed for the molybdenum samples, an increase of the reflectivity is measured for the sample with 15 nm of Be. The layer in this case appears to be highly reflective and has a light gray color. Indications of diffusion of Be into the Cu bulk have been given by Rutherford backscattering spectroscopy measurements performed on the samples.

Previous studies[20,21] showed that already at 300 °C, diffusion of Be into Cu may be expected, as well as formation of BeCu, or Be_2Cu, alloys. The enhancement of the reflectivity shown in Fig. 4(b), as well as the peculiar aspect of the associated layer may, therefore, be attributed to the formation of a copper-beryllium alloy on the surface, the stoichiometry of the alloy was not investigated, however.

For the other two samples (with 55 and 75 nm thick films), though diffusion of Be into Cu was also evidenced at the film-substrate interface, the layers have the same appearance as those described for the molybdenum mirrors. Correspondingly, a significant decrease of the mirror reflectivity due to Be deposition is measured. Moreover, the reflectivity of these two samples is significantly lower than the reflectiv-

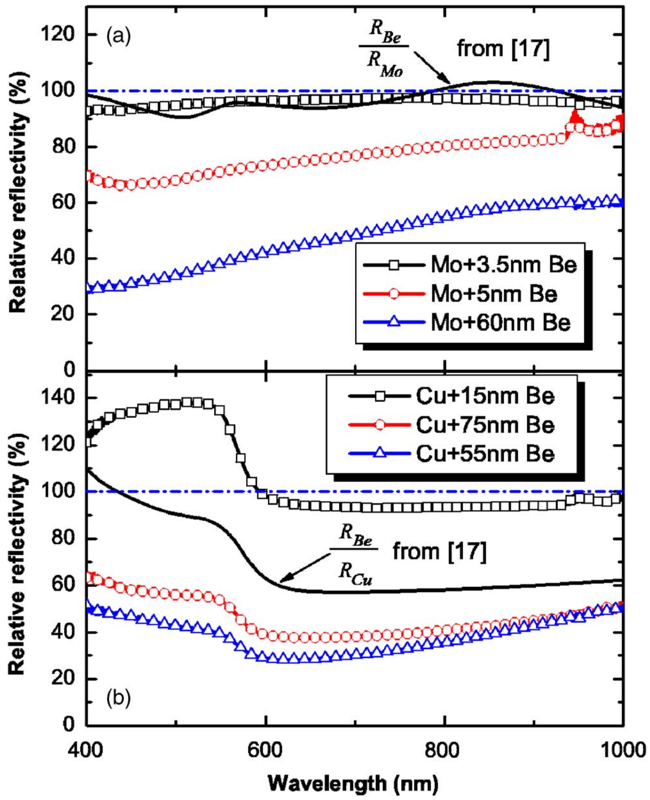

FIG. 4. (Color online) Relative reflectivity of Be deposits on (a) molybdenum and (b) copper mirrors. Mirrors were heated to 300 °C during the exposure. For both graphs the black line corresponds to the relative reflectivity of Be and Mo or Be and Cu taken from Ref. 19 and corresponds to the reflectivity which should be measured if the mirror consisted of a perfectly smooth Be layer deposited on the respective polished substrates. The dashed line at 100% indicates the reference level (corresponding to a nonexposed sample).

ity of pure beryllium. In this case, however, and contrary to what was described for molybdenum, the thickest film (75 nm) does not exhibit the lowest reflectivity.

From these results one can already conclude that the reflectivity of the Be layers formed in PISCES-B is much lower than the values expected for a pure Be surface, despite the low level of impurities found in the film.

C. Morphology of the Be layers

As mentioned, the impurity content in the layers cannot account for the drastic changes of the reflectivity induced by beryllium deposition on the mirrors. From Table I, we can also infer that the reflectivity losses are not caused by an increase of the surface roughness after exposure. To shed some light on the reflectivity measurements, the morphology of the samples was investigated using SEM. Figure 5 shows the SEM images obtained at two different magnifications on copper and tungsten mirrors, exposed at 240 °C. Pictures with the lower magnifications reveal quite different features. The surface of the copper mirror [Fig. 5(a)] appears relatively smooth, which is confirmed by the roughness determined with the profilometer (~16 nm). One should, however, mention that even at this magnification, some morphology can be distinguished on the surface. On the contrary, lots of protuberances can be observed on the surface of

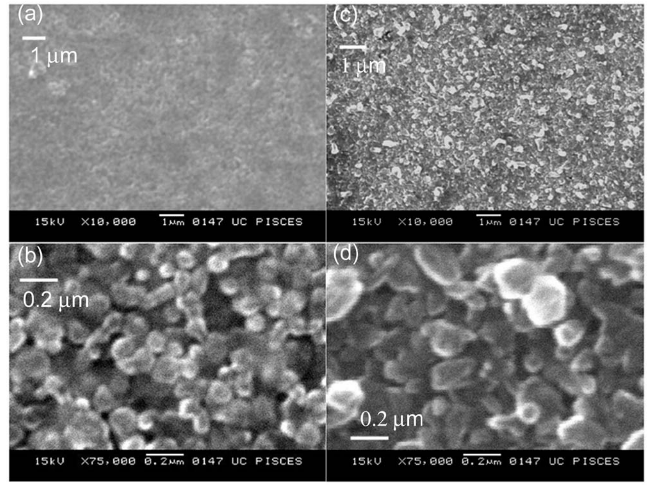

FIG. 5. SEM pictures of Be layers deposited on copper [(a) and (b)] and tungsten [(c) and (d)]. Film thicknesses are 75 and 90 nm, respectively. For each case two different magnifications are shown.

the tungsten sample [Fig. 5(c)]. This observation is in good agreement with the higher roughness (~41 nm) measured for the tungsten sample after exposure. Pictures taken at higher magnification reveal a high layer porosity on both samples. The layers appear to be made of small-size crystallites separated by voids. Although estimations of the depth distribution of the porosity throughout the layer is difficult from the SEM pictures, it seems nevertheless that the distribution is homogeneous and the porosity is not only present on the top surface of the film but also in the bulk of the layer.

Similar observations are made for samples exposed at lower temperature (at room temperature at the beginning of the exposure). Layers observed on both substrates have the same structure, although the crystallite size appears slightly higher in the case of tungsten. Such structures are quite similar to the "spongelike" structure described in Refs. 22 and 23, which refers to a polycrystal with continuous open porosity, but without the definitive columnar features characteristic of the classic structure zone models.

IV. DISCUSSION

A. Influence of the film porosity on the optical properties

Considering the SEM pictures described before, and the facts that no significant increase of the roughness is observed after beryllium deposition and that the impurity content in the Be films is relatively low, suggests that the low reflectivity values measured on the exposed samples are caused by the high porosity of the layers. Moreover, preparation of porous Be coatings was reported in Ref. 24. In that study, the porosity was found to strongly decrease the coating reflectivity. It is commonly acknowledged that the optical properties of a porous material can be described using an effective medium approximation, in which the heterogeneous material is treated as a homogeneous material with effective optical properties.[25,26]

Although different approaches exist with their own validity domain and approximations, it was chosen here to use the Bruggeman effective approximation.[27] Bruggeman's theory is based on the assumption of polydispersed spheres distributed in a continuous medium. In the present case, we consider the porous film to consist in a mixture of beryllium and air. For the calculation of the effective dielectric function, $\tilde{\epsilon}_{\text{eff}}$, of the inhomogeneous medium the Bruggeman theory offers the following equation:

$$f\frac{\tilde{\epsilon}_{\text{air}}-\tilde{\epsilon}_{\text{eff}}}{\tilde{\epsilon}_{\text{air}}+2\tilde{\epsilon}_{\text{eff}}}+(1-f)\frac{\tilde{\epsilon}_{\text{Be}}-\tilde{\epsilon}_{\text{eff}}}{\tilde{\epsilon}_{\text{Be}}+2\tilde{\epsilon}_{\text{eff}}}=0, \tag{2}$$

where $\tilde{\epsilon}_{\text{eff}}$, $\tilde{\epsilon}_{\text{air}}$, and $\tilde{\epsilon}_{\text{Be}}$ are the dielectric constants of the porous film, air, and beryllium, respectively. Optical properties of beryllium and air are taken from Ref. 19. f is the porosity of the film and can be defined as the volumetric fraction of air in the film

$$f=\frac{\text{air volume}}{\text{film volume}}=\frac{\text{air volume}}{\text{air volume}+\text{Be volume}}. \tag{3}$$

The dielectric constant is a complex function and can be written as $\tilde{\epsilon}=\epsilon_1+i\epsilon_2$. For different values of f, ranging from 0% to 100%, the effective dielectric constant of a 75 nm thick Be film deposited on copper was calculated. The following equations were then used to determine the effective optical constants of the film:

$$n^2-k^2=\epsilon_1,$$

$$2nk=\frac{\epsilon_2}{\sqrt{2}}, \tag{4}$$

where n and k are the refractive and absorption index, respectively.

The reflectivity of the effective medium at normal incidence was then recalculated, roughness of both the film and the substrate being neglected. Figure 6(a) shows the evolution of the optical properties of the film at $\lambda=632$ nm. As expected, optical constants of the film decrease with increasing film porosity and tend to the optical constants of air. As a result the reflectivity of the film decreases for increasing porosity [Fig. 6(b)]. A porosity of 50% decreases the reflectivity of a Be layer to about 30% in the wavelength range 350–1200 nm. It should be noted that the effect of the porosity on the reflectivity is slightly less pronounced for wavelengths higher than 1400 nm.

Figure 7 shows the relative reflectivity of a Be layer (i.e., the reflectivity of the system Be+Cu divided by the reflectivity of Cu) deposited on a copper substrate for different values of the film porosity. As just mentioned, the porosity decreases the relative reflectivity of the layer. Also plotted in Fig. 7 is the relative reflectivity of a Cu mirror exposed in PISCES-B and coated with a 75 nm thick Be layer, whose morphology is shown in Figs. 5(a) and 5(b). Evidently, the shape of the experimental reflectivity spectrum is very close to those simulated from the effective medium approximation. This suggests that the relatively high porosity of the layers formed in PISCES-B is the reason for the low reflectivity values measured experimentally. Moreover, the experimental reflectivity spectrum lies between the simulated spectra obtained for $f=40\%$ and $f=50\%$, giving a rough estimate of the

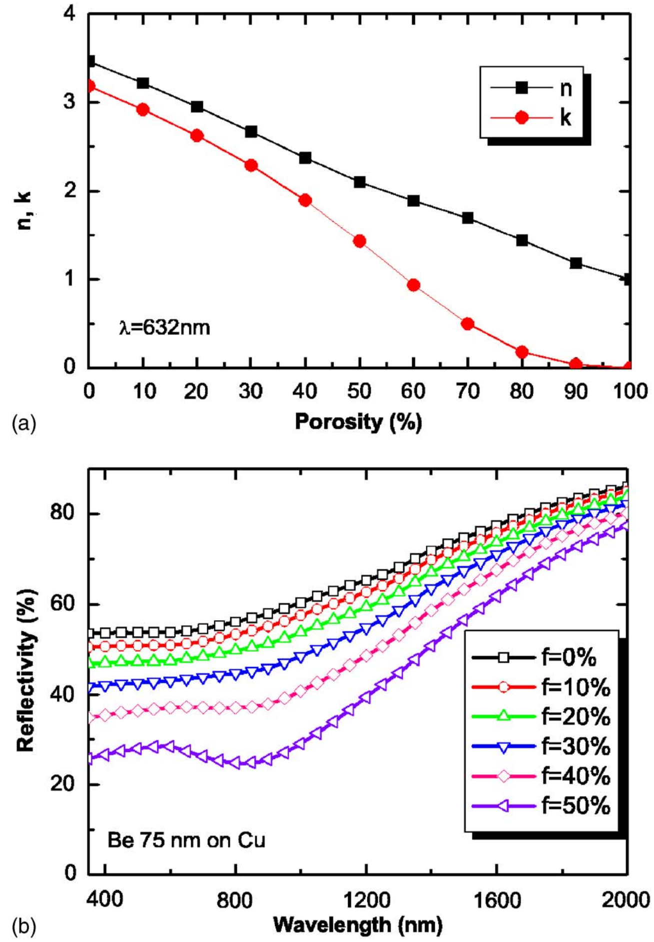

FIG. 6. (Color online) (a) Optical constants (n,k) at 632 nm of the effective medium (air+beryllium) used to describe a porous Be film deposited on a Cu substrate (film thickness 75 nm) as a function of the film porosity (using the Bruggeman effective approximation) and (b) reflectivity at normal incidence of the effective medium in the wavelength range 350–2000 nm for different values of the film porosity.

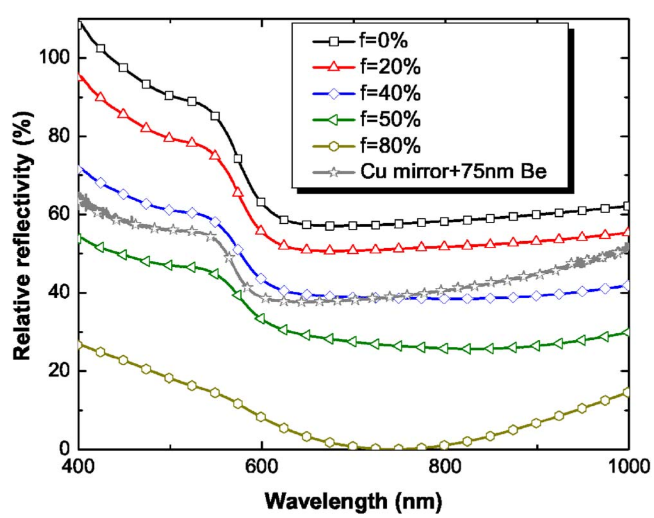

FIG. 7. (Color online) Calculated relative reflectivity of a Be layer deposited on a copper substrate for different values of the film porosity. Also plotted (gray line with star markers) is the experimentally measured relative reflectivity of a copper mirror exposed in PISCES-B and coated with a 75 nm thick Be layer.

porosity of the Be film deposited in PISCES-B. Based on observation of Fig. 5(b), it seems that this estimation is reasonable.

B. Formation of porous layers and implications for ITER

Formation mechanisms of thin films in vacuum deposition techniques, magnetron sputtering for example, have been widely studied. Though PISCES-B has been designed to study plasma-surface interactions, the way in which Be films are formed on the witness plate is quite similar to what happens in a magnetron sputtering system. Indeed, in both cases, material from a negatively biased target is eroded by the plasma ions and redeposited on the witness plate. We may, therefore, make use of the extensive literature describing film formation by physical vapor deposition (PVD), keeping in mind that in our case deuterium is used as a working gas (instead of noble gases like argon in PVD techniques).

The structure of a vacuum-deposited film depends on the substrate temperature, the working gas pressure, and the incident particle fluxes.[28] Effects of pressure and temperature on the film morphology are qualitatively explained by the structure zone model described in Ref. 29. To describe the effect of the temperature, it is common to use the ratio T/T_m of the temperature during deposition to the melting temperature of the deposited material (beryllium here). For values of $T/T_m \leq 0.3$ (which is the case in the experiments described here), the film porosity is found to increase for increasing values of the working gas pressure.[28] This is explained by the reduction in surface mobility of the deposited atoms caused by the higher density of working gas atoms on the surface at higher pressures.[30] In the case of the beryllium layers formed in PISCES-B, a significant level of porosity is measured for neutral pressures of 0.5–0.8 Pa during deposition, while the ratio T/T_m of the temperature during deposition to the melting temperature of beryllium remains lower than 0.25. Thus, keeping the same temperature, but decreasing the pressure during deposition should lower the level of porosity, while increasing it should produce more porous layers.

Although Be deposition will modify the mirror reflectivity in ITER, the actual reflectivity of the coated mirrors will depend on the layer morphology. Of particular importance seems to be the layer porosity, which makes the reflectivity of the Be layers formed in PISCES-B much lower than the reflectivity of pure Be. In ITER, mirrors will be installed at several locations in the main chamber (recessed behind the first wall) and in the divertor region. Estimations of the neutral pressure in ITER rely on numerical models and/or scaling laws. According to these calculations the pressure in the ITER divertor may reach 10 Pa.[1,31] No such data exist for the neutral pressure in the main chamber, but one can consider that the neutral pressure in the main chamber will be linked to the local charge-exchange neutral outflux, which is itself linked to the local density and divertor leakage.[32] The charge-exchange outfluxes and energy distribution in ITER may be quite close to those in JET,[33] where the typical upstream midplane pressure for a high density *L*-mode discharge is in the range 0.05 Pa.[34] From these estimations, one sees that the pressure in the ITER divertor will be higher thanin PISCES-B and if Be deposition occurs on the mirrors located in the divertor, a high level of porosity may be expected. On the contrary, lower pressure in the main chamber may lead to the formation of more dense layers, which in turn may lead to layers whose reflectivity may be expected to be closer to that of beryllium.

V. CONCLUSION

The formation of beryllium layers on mirrors exposed in PISCES-B was found to strongly affect the mirror reflectivity. The most striking feature was that the reflectivity of the Be layers are much lower than what was expected for a pure Be sample, despite the relatively low levels of impurities. Investigations of the layer morphology revealed a high level of porosity. Calculations using the Bruggemann effective medium approximations confirmed that the relatively high porosity of the layers is the reason for the low reflectivity values measured experimentally.

If Be deposition occurs on ITER first mirrors, the mirror reflectivity will depend strongly on the morphology of the deposited layer which, in turn, is linked to the deposition conditions (temperature, neutral pressure) at the mirror location. Extrapolations from the present results to the ITER conditions indicate that Be layers formed in the divertor region may exhibit significant levels of porosity because of the high neutral pressure in this region. On the other hand, the lower pressure expected in the main chamber may lead to the formation of more dense layers, whose reflectivity is expected to be closer to the theoretical value of beryllium.

ACKNOWLEDGMENTS

The authors gratefully acknowledge the help and support from the PISCES-B technical staff, as well as fruitful discussions with Dr. R. A. Pitts. This work was supported by the U.S. Department of Energy under Contract No. DE-FG02-07ER54912 and by the U.S.-EU bilateral collaboration on mixed materials.

[1]ITER Physics Basis, Nucl. Fusion **47** (2007).
[2]A. Costley, D. J. Campbell, S. Kasai, K. E. Young, and V. Zaveriaev, Fusion Eng. Des. **55**, 331 (2001).
[3]V. S. Voitsenya, A. E. Costley, V. Bandourko, A. Bardamid, V. Bondarenko, Y. Hirooka, S. Kasai, N. Klassen, V. Konovalov, M. Nagatsu, K. Nakamura, D. Orlinskij, F. Orsitto, L. Poperenko, S. Solodovchenko, A. Stan, T. Sugie, M. Taniguchi, M. Vinnichenko, K. Vukolov, and S. Zvonkov, Rev. Sci. Instrum. **72**, 475 (2001).
[4]A. Litnovsky, P. Wienhold, V. Philipps, G. Sergienko, O. Schmitz, A. Kirschner, A. Kreter, S. Droste, U. Samm, Ph. Mertens, A. H. Donne, D. Rudakov, S. Allen, R. Boivin, A. McLean, P. Stangeby, W. West, C. Wong, M. Lipa, B. Schunke, G. De Temmerman, R. A. Pitts, A. Costley, V. Voitsenya, K. Vukolov, P. Oelhafen, M. Rubel, and A. Romanyuk, J. Nucl. Mater. **363–365**, 1395 (2007).
[5]V. S. Voitsenya, A. F. Bardamid, V. N. Bondarenko, W. Jacob, V. G. Konovalov, S. Masuzaki, O. Motojima, D. V. Orliskij, V. L. Poperenko, I. V. Ryzhkov, A. Sagara, A. F. Shtan, S. I. Solodovchenko, and M. V. Vinnichenko, J. Nucl. Mater. **290–293**, 336 (2001).
[6]T. Sugie, S. Kasai, M. Taniguchi, M. Nagatsu, and T. Nishitani, J. Nucl. Mater. **329–333**, 1481 (2004).
[7]G. De Temmerman, R. A. Pitts, V. S. Voitsenya, L. Marot, G. Veres, M. Maurer, and P. Oelhafen, J. Nucl. Mater. **363–365**, 259 (2007).
[8]M. Lipa, B. Schunke, Ch. Gil, J. Bucalossi, V. S. Voitsenya, V. Konovalov, K. Vukolov, M. Balden, G. De Temmerman, P. Oelhafen, A. Litnovsky,

and P. Wienhold, Fusion Eng. Des. **81**, 221 (2006).

[9] A. Litnovsky, G. De Temmerman, K. Vukolov, P. Wienhold, V. Philipps, O. Schmitz, U. Samm, G. Sergienko, P. Oelhafen, M. Buttner, I. Orlovskiy, A. Yastrebkov, U. Breuer, and A. Scholl, Fusion Eng. Des. **82**, 123 (2007).

[10] G. De Temmerman and R. A. Pitts, Fusion Eng. Des. (2007).

[11] G. Federici and C. H. Skinner, *Nuclear Fusion Research: Understanding Plasma-Surface Interactions*, Springer Series in Chemical Physics (Springer, New York, 2004).

[12] K. Schmid, M. Baldwin, R. Doerner, and A. Wiltner, Nucl. Fusion **44**, 815 (2004).

[13] M. J. Baldwin, K. Schmid, R. P. Doerner, A. Wiltner, R. Seraydarian, and Ch. Linsmeier, J. Nucl. Mater. **337–339**, 590 (2005).

[14] M. J. Rubel, G. De Temmerman, J. P. Coad, J. Vince, J. R. Drake, F. Le Guern, A. Murari, R. A. Pitts, C. Walker, and JET-EFDA contributors, Rev. Sci. Instrum. **77**, 063501 (2006).

[15] R. Doerner and C. Mays, Fusion Eng. Des. **37**, 325 (1997).

[16] R.P. Doerner, M.J. Baldwin, and K. Schmid, Phys. Scr., T **T111**, 75 (2004).

[17] D. G. Whyte, G. R. Tynan, R. P. Doerner, and J. N. Brooks, Nucl. Fusion **41**, 47 (2001).

[18] M. Balden and J. Roth, J. Nucl. Mater. **280**, 39 (2000).

[19] *Handbook of Optical Constants of Solid*, 1st ed., edited by E. D. Palik (Academic, New York, 1985); *Handbook of Optical Constants of Solids*, 2nd ed., edited by E. D. Palik (Academic, New York, 1991).

[20] H. Kawamura and M. Kato, Proceedings of the 2nd IEA International Workshop Beryllium Technology for Fusion, Jackson Lake Lodge, WY, 6–8 September 1995, p. 204 (unpublished).

[21] B. C. Odegard, Jr., C. H. Cadden, and N. Y. C. Yang, Fusion Eng. Des. **41**, 63 (1998).

[22] A. F. Jankowski and J. P. Hayes, J. Vac. Sci. Technol. A **21**, 422 (2003).

[23] R. J. Burt, S. F. Meyer, and E. J. Hsieh, J. Vac. Sci. Technol. **17**, 407 (1980).

[24] C. M. Egert and D. D. Allred, *SPIE Stray Radiation in Optical Systems* (SPIE, Bellingham, WA, 1990), Vol. 1331, p. 170.

[25] M. T. Othman, J. A. Lubguban, A. A. Lubguban, S. Gangopadhyay, R. D. Miller, W. Volksen, and H. C. Kim, J. Appl. Phys. **99**, 083503 (2006).

[26] M. Braun and L. Pilon, Thin Solid Films **496**, 505 (2006).

[27] D. A. G. Bruggeman, Ann. Phys. **24**, 636 (1935).

[28] J. A. Thornton, J. Vac. Sci. Technol. **11**, 666 (1979).

[29] B. A. Movchan and A. V. Demchishin, Phys. Met. Metallogr. **28**, 83 (1969).

[30] W. D. Westwood, J. Vac. Sci. Technol. **11**, 466 (1974).

[31] A. S. Kukushkin, H. D. Pacher, G. W. Pacher, G. Janseschitz, D. Coster, A. Loarte, and D. Reiter, Nucl. Fusion **43**, 716 (2003).

[32] R. A. Pitts (private communication).

[33] R. A. Pitts, J. P. Coad, D. P. Coster, G. Federici, W. Fundamenski, J. Horacek, K. Krieger, A. Kukushkin, J. Likonen, G. F. Matthews, M. Rubel, J. D. Strachan, and JET-EFDA contributors, Plasma Phys. Controlled Fusion **47**, B303 (2005).

[34] R. A. Pitts, P. Andrew, X. Bonnin, A. V. Chankin, Y. Corre, G. Corrigan, D. Coster, I. Duran, T. Eich, S. K. Erents, W. Fundamenski, A. Huber, S. Jachmich, G. Kirnev, M. Lehnen, P. J. Lomas, A. Loarte, G. F. Matthews, J. Rapp, C. Silva, M. F. Stamp, J. D. Strachan, F. Tsitrone, and contributors to the EFDA-JET workprogramme, J. Nucl. Mater. **313–316**, 777 (2003).